The American Journal of Human Genetics, Volume *108*

Supplemental information

Bi-allelic mutations of *DNAH10* cause primary male infertility with asthenoteratozoospermia in humans and mice

Chaofeng Tu, Jiangshan Cong, Qianjun Zhang, Xiaojin He, Rui Zheng, Xiaoxuan Yang, Yang Gao, Huan Wu, Mingrong Lv, Yayun Gu, Shuai Lu, Chunyu Liu, Shixiong Tian, Lanlan Meng, Weili Wang, Chen Tan, Hongchuan Nie, Dongyan Li, Huan Zhang, Fei Gong, Liang Hu, Guangxiu Lu, Wenming Xu, Ge Lin, Feng Zhang, Yunxia Cao, and Yue-Qiu Tan

Supplemental Note: Case Reports

All individuals presented with typical MMAF phenotypes characterized by multiple flagellar malformations, including absent, short, coiled, bent, and/or irregular-caliber flagella. Subjects with evident PCD-related symptoms,[1] such as recurrent airway inflammation, bronchiectasis, and otitis media, were excluded. Individuals presenting with other causes of infertility, such as reproductive malformation, drug use, and exposure to gonadotoxic factors, were also excluded. No abnormalities were detected with regard to somatic chromosomal karyotypes and Y chromosome microdeletions. The study was approved by the ethics committees of all participating institutes. Informed consent was obtained from all participants at the beginning of the study.

Supplemental References

1. Knowles, M.R., Zariwala, M., and Leigh, M. (2016). Primary Ciliary Dyskinesia. Clin. Chest Med. 37, 449-461.

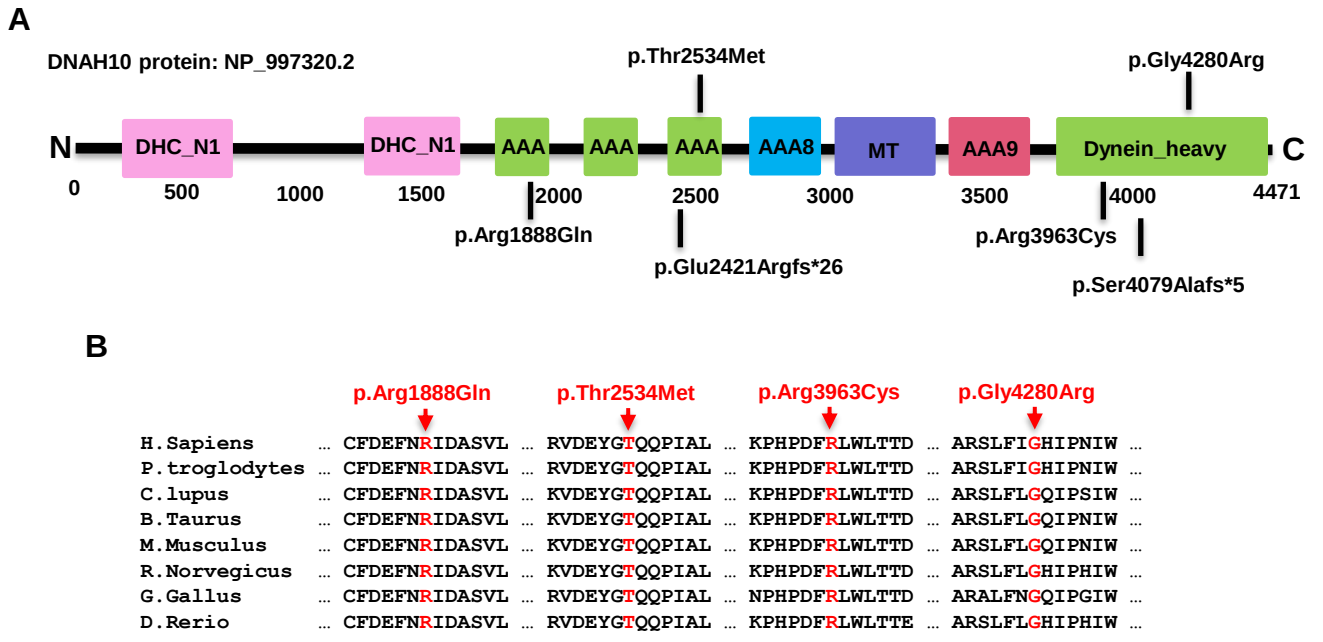

Figure S1. Phylogenetic Conservation of the Mutated Residues in DNAH10 Protein

(A) The positions of six variants in *DNAH10* identified in male cases with asthenoteratozoospermia are shown. Domains/motifs in DNAH10 are indicated in different colored squares according to the NCBI browser.

(B) Sequence alignment shows that the four detected *DNAH10* missense variants are conserved among different species.

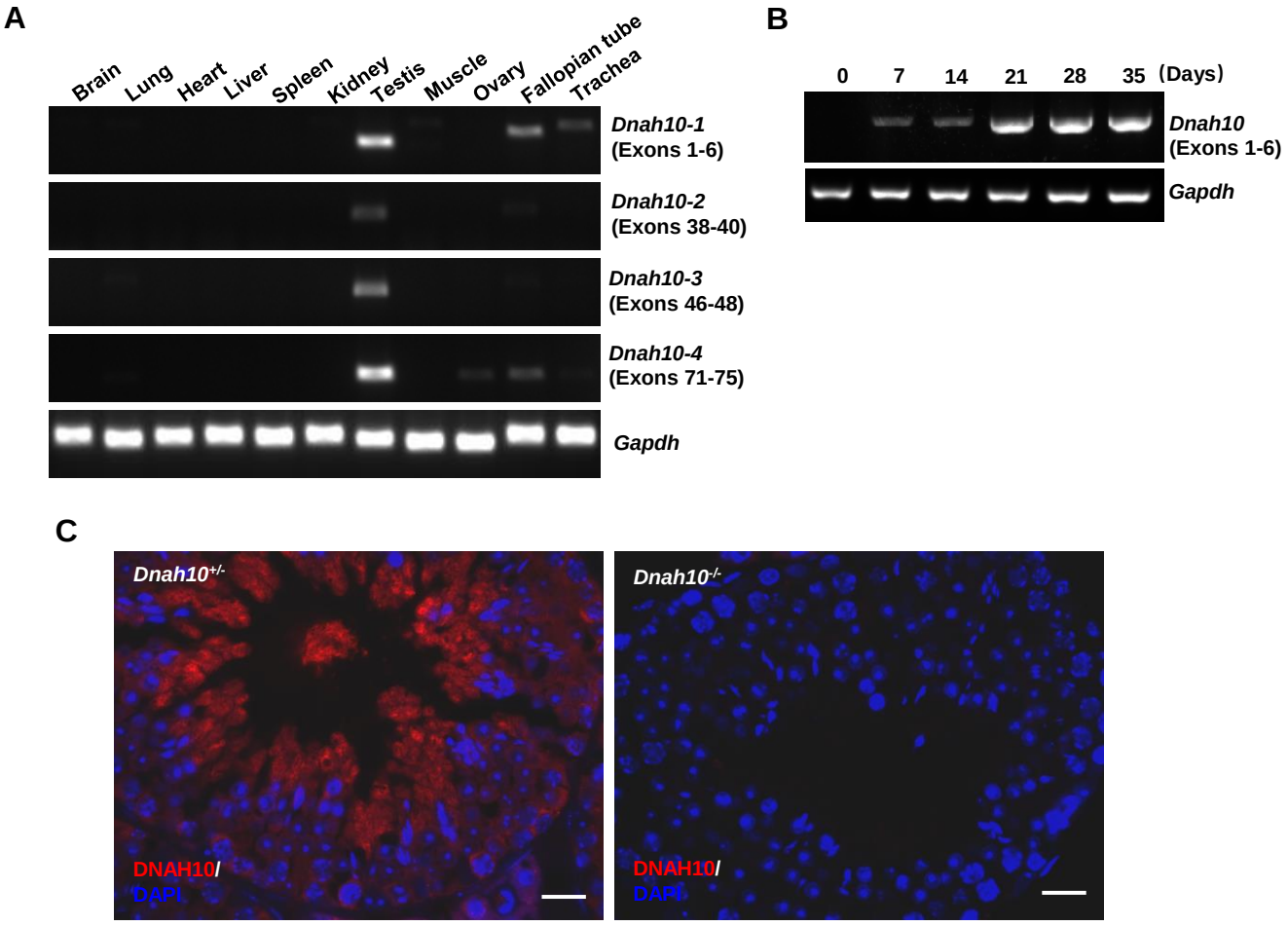

Figure S2. Gene Expression of *Dnah10* in Different Mouse Tissues.

(A) Expressions of *Dnah10* were investigated by RT-PCR in various tissues from adult male mice. *Gapdh* was used as an internal control.

(B) The expression of mouse *Dnah10* mRNA in the testis was highly elevated from postnatal day 21, corresponding to the spermiogenesis stage. Gapdh was as an internal control.

(C) Representative image of testicular tubules stained with anti-DNAH10 antibody and DAPI showing that DNAH10 is localized in the cytoplasm of elongated spermatozoa in the testis from *Dnah10*$^{+/-}$ male mice, but was almost absent in *Dnah10*$^{-/-}$ male mice. Scale bars = 50 μm.

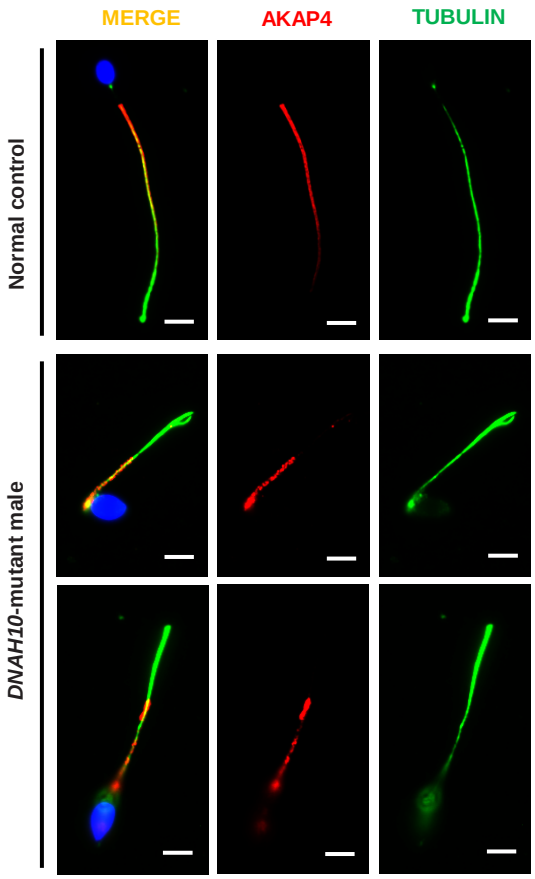

Figure S3. Immunofluorescence Staining of AKAP4 in the Spermatozoa from a Fertile Male Control and Men Harboring Bi-allelic *DNAH10* Variants.

Sperm cells were stained with anti-AKAP4 (red) and anti-α-tubulin (green) antibodies, respectively. DNA was counterstained with DAPI as a marker of the cell nucleus. The AKAP4 signaling in the sperm flagella of individuals with bi-allelic *DNAH10* variants is mislocalized along the sperm tail. Scale bars: 5 µm.

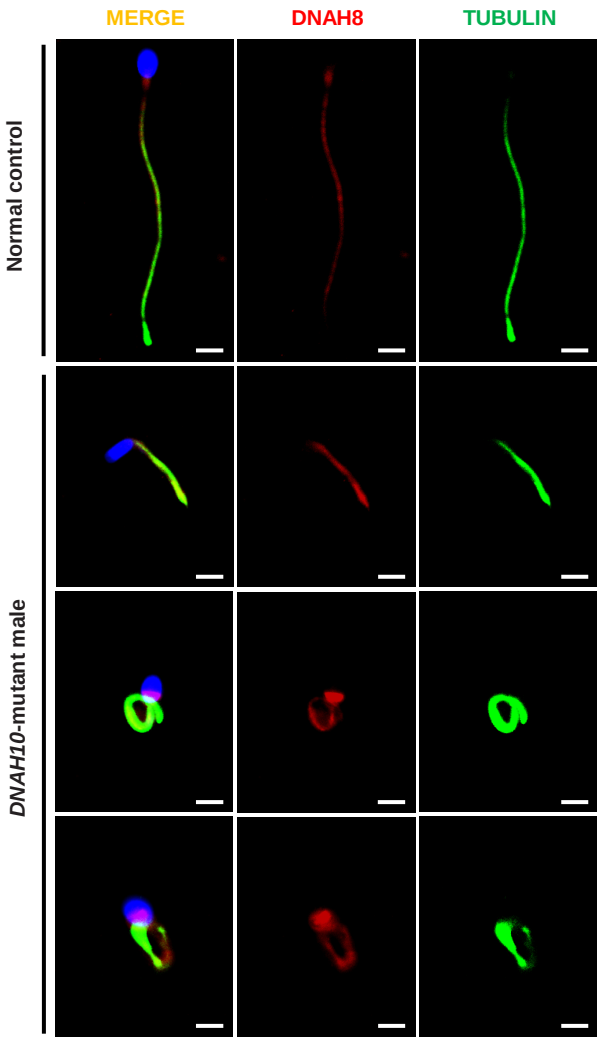

Figure S4. Immunofluorescence Staining of DNAH8 in the Spermatozoa from a Fertile Male Control and Men Harboring Bi-allelic *DNAH10* Variants.

Sperm cells were stained with anti-DNAH8 (red) and anti-α-tubulin (green) antibodies. DNA was counterstained with DAPI as a marker of the cell nucleus. DNAH8 staining is concentrated at the sperm flagella from the normal control and the signal in the *DNAH10*-mutant group is comparable with that of controls. Scale bars: 5 µm.

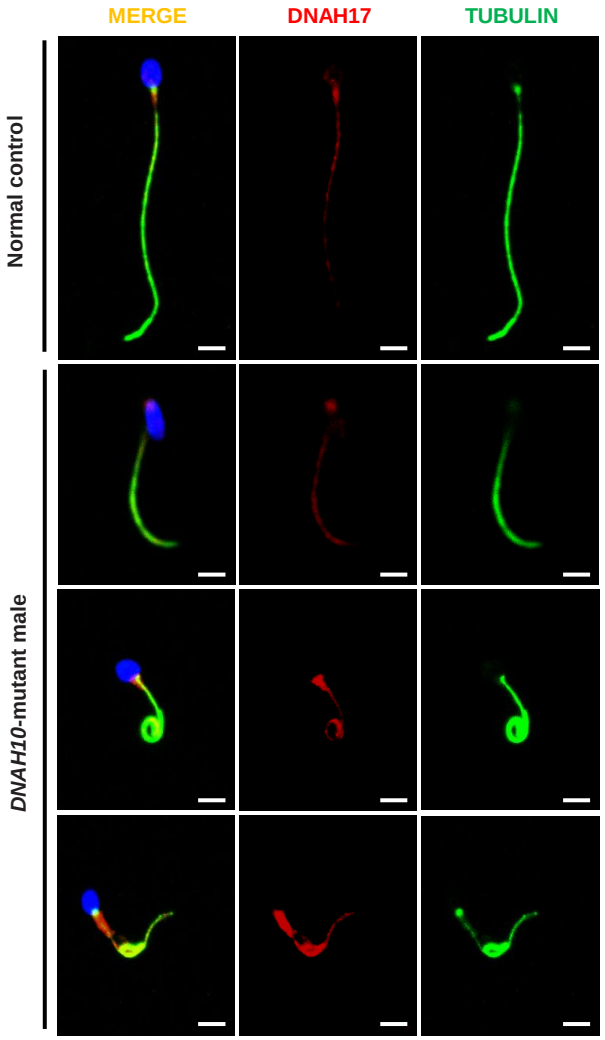

Figure S5. Immunofluorescence Staining of DNAH17 in the Spermatozoa from a Fertile Male Control and Men Harboring Bi-allelic *DNAH10* Variants.

Sperm cells were stained with anti-DNAH17 (red) and anti-α-tubulin (green) antibodies. DNA was counterstained with DAPI as a marker of the cell nucleus. DNAH17 staining is concentrated at the sperm flagella from the normal control and the signal in the *DNAH10*-mutant group is comparable with that of controls. Scale bars: 5 μm.

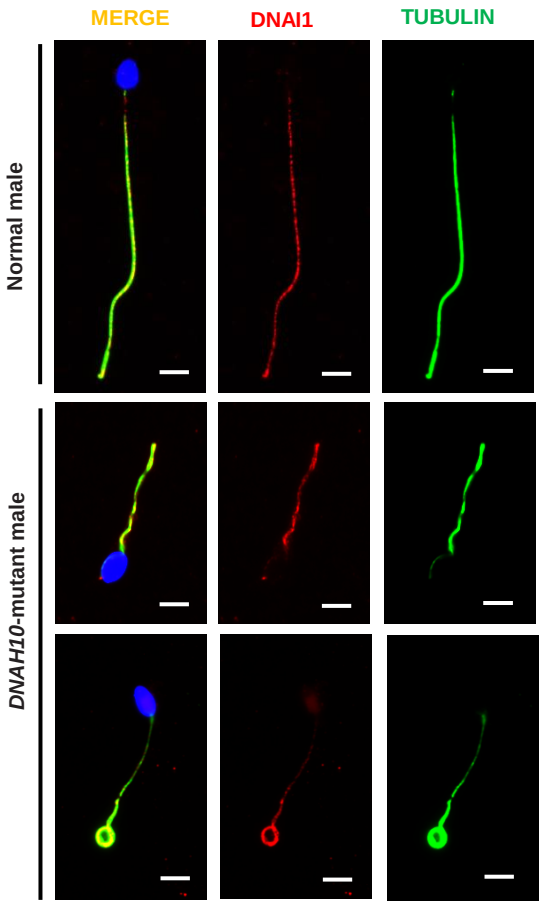

Figure S6. Immunofluorescence Staining of DNAI1 in the Spermatozoa from a Fertile Male Control and Men Harboring Bi-allelic *DNAH10* Variants.

Sperm cells were stained with anti-DNAI1 (red) and anti-α-tubulin (green) antibodies. DNA was counterstained with DAPI as a marker of the cell nucleus. DNAI1 staining is concentrated at the sperm flagella from the normal control and the signal in the *DNAH10*-mutant group is comparable with that of controls. Scale bars: 5 μm.

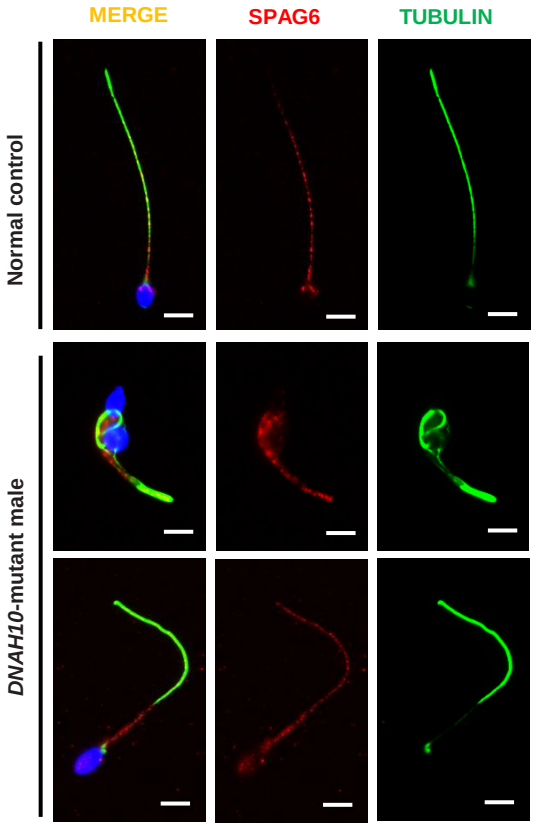

Figure S7. Immunofluorescence Staining of SPAG6 in the Spermatozoa from a Fertile Male Control and Men Harboring Bi-allelic *DNAH10* Variants.

Sperm cells were stained with anti-SPAG6 (red) and anti-α-tubulin (green) antibodies. DNA was counterstained with DAPI as a marker of the cell nucleus. The signal in the *DNAH10*-mutant group is comparable with that of controls, suggesting that central pair was not directly affected by bi-allelic *DNAH10* Variant. Scale bars: 5 μm.

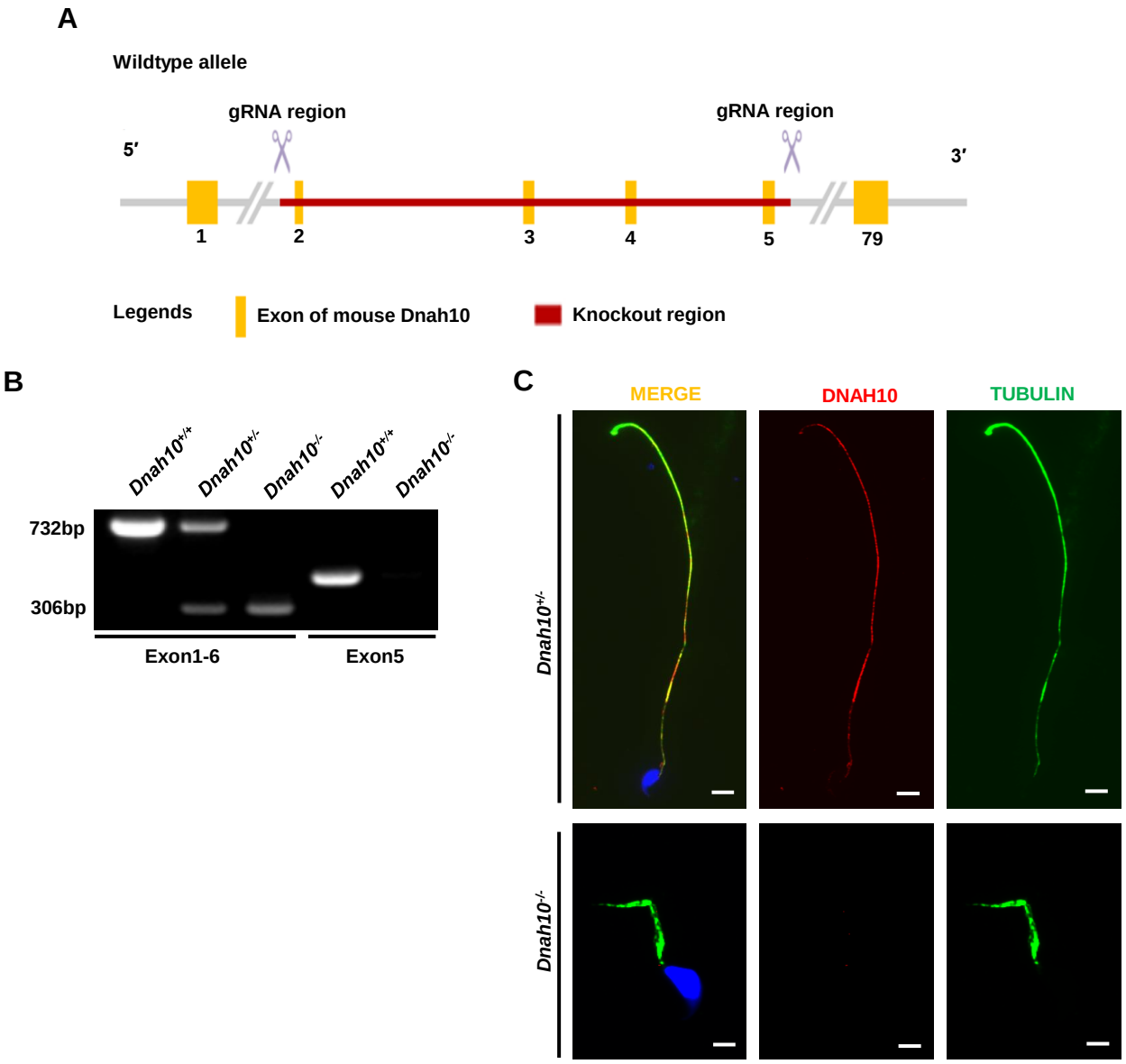

Figure S8. Schematic Illustration of the Targeting Strategy for Generating *Dnah10*$^{-/-}$ Mice

(A) The *Dnah10* knockout strategy in mice. The gRNAs were targeted in exons 2 and 5 of mouse *Dnah10* to delete the partial coding region.

(B) RT-PCR of mRNA isolated from *Dnah10*$^{+/+}$, *Dnah10*$^{+/-}$ and *Dnah10*$^{-/-}$ male mice testes indicated the presence of a truncated transcript in *Dnah10*$^{-/-}$ male mice testes using the *Dnah10* primers which located exon 1 to exon 6 and exon 5, respectively.

(C) DNAH10 (red, specifically binding human amino acids 3561-3700) localized at the entire flagella in the sperm of *Dnah10*$^{+/-}$ male mice. In contrast, DNAH10 staining was absent in the sperm of *Dnah10*$^{-/-}$ male mice. Tubulin indicated the flagella (green), and the nuclei of spermatozoa were counterstained with DAPI (blue). Scale bars = 10 mm.

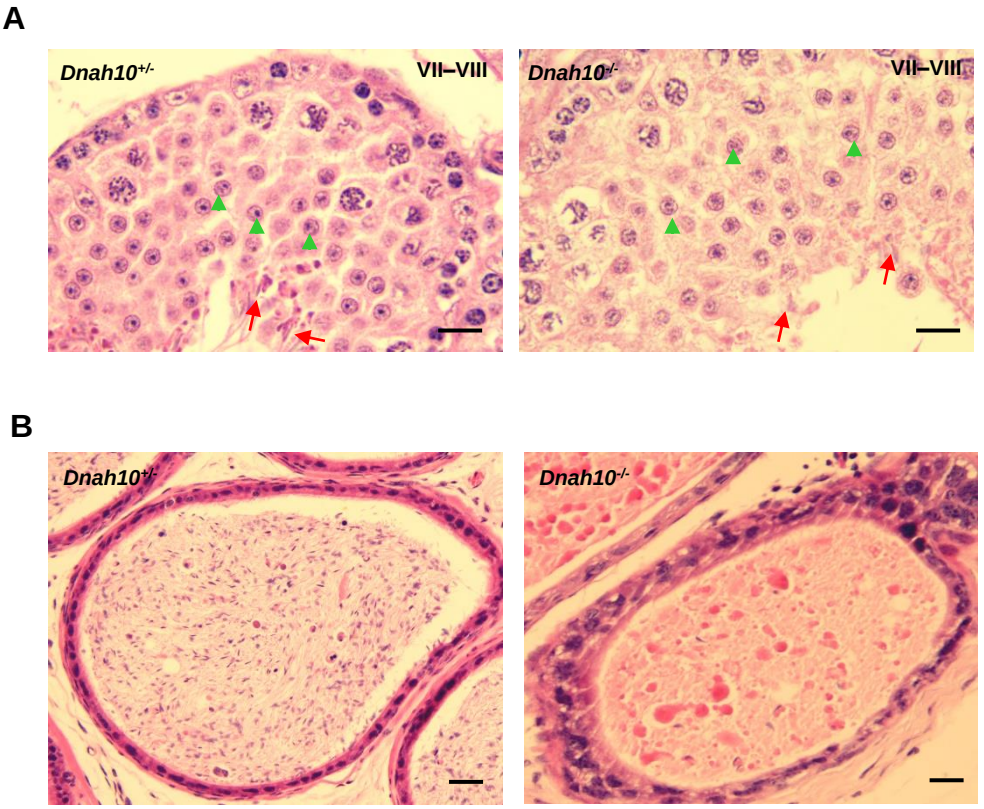

Figure S9. Histological Examinations of Testes and Epididymides from *Dnah10*$^{+/-}$ and *Dnah10*$^{-/-}$ Male Mice

(A) H&E staining of testicular tissues in *Dnah10*$^{-/-}$ male mice and *Dnah10*$^{+/-}$ male mice at 2-month-old. In stage VII–VIII seminiferous tubules from *Dnah10*$^{-/-}$ male mice, normal round spermatids (green, arrowheads) were observed, but the morphology of elongated tails (red arrows) were abnormal. Scale bars = 20 μm.

(B) H&E staining of testicular epididymal sections in *Dnah10*$^{-/-}$ male mice and *Dnah10*$^{+/-}$ male mice at 2-month-old. Compared with *Dnah10*$^{+/-}$ male mice, sperm counts were obviously decreased in the epididymis from *Dnah10*$^{-/-}$ male mice. Scale bars = 20 μm.

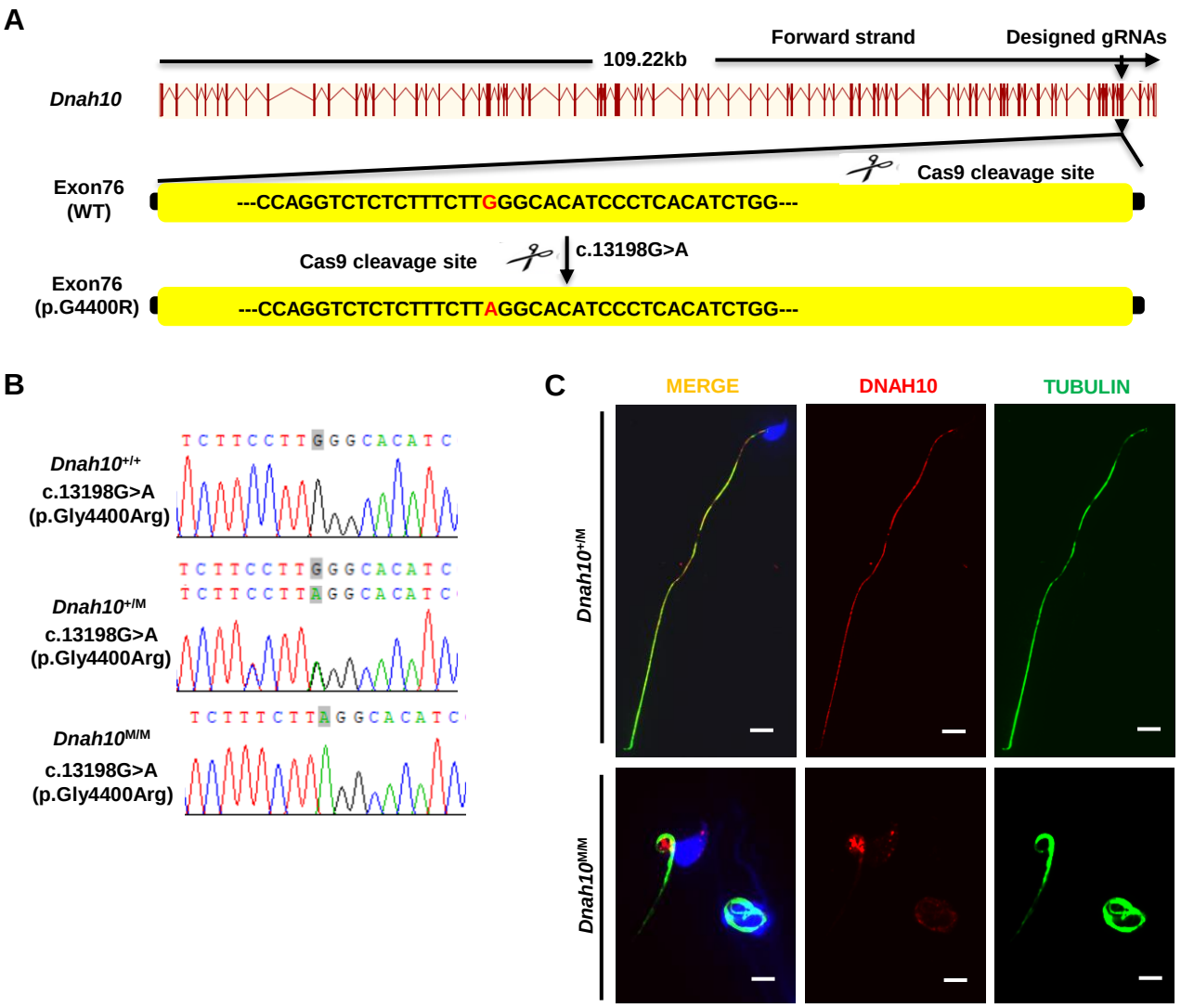

Figure S10. Schematic Illustration of the Targeting Strategy for Generating *Dnah10*$^{M/M}$ Mice

(A) Schematic illustrating construction of the knockin mouse model (*Dnah10*$^{M/M}$). A gRNA was designed targeting exon 76 of *Dnah10*. The mutated nucleotides in mice (c.13198G>A) equivalent to that in *DNAH10*-mutant patient T012 II-2 (c.12838G>A) are written in red.

(B) Sanger sequencing showing the c.13198G>A mutation heterozygous in *Dnah10*$^{+/M}$ and homozygous in *Dnah10*$^{M/M}$ mice.

(C) DNAH10 (red) localized at the entire flagella in the sperm of *Dnah10*$^{+/M}$ male mice. In contrast, DNAH10 staining was reduced in the sperm of *Dnah10*$^{M/M}$ male mice. Tubulin indicated the flagella (green), and the nuclei of spermatozoa were counterstained with DAPI (blue). Scale bars = 10 mm.

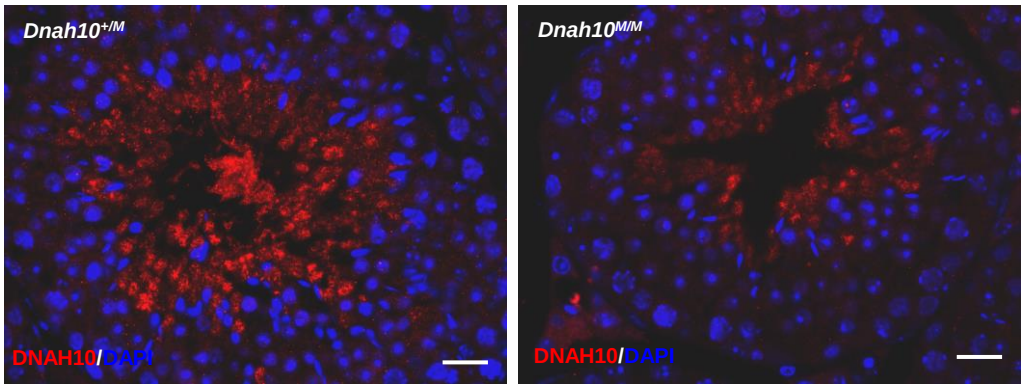

Figure S11. Immunostaining of *Dnah10* in testis from *Dnah10*$^{M/M}$ male mice.

Representative image of testicular tubules stained with anti-DNAH10 antibody and DAPI showing that DNAH10 is localized in the cytoplasm of elongated spermatozoa in the testis from *Dnah10*$^{+/M}$ male mice, but was reduced in *Dnah10*$^{M/M}$ male mice. Scale bars = 50 μm.

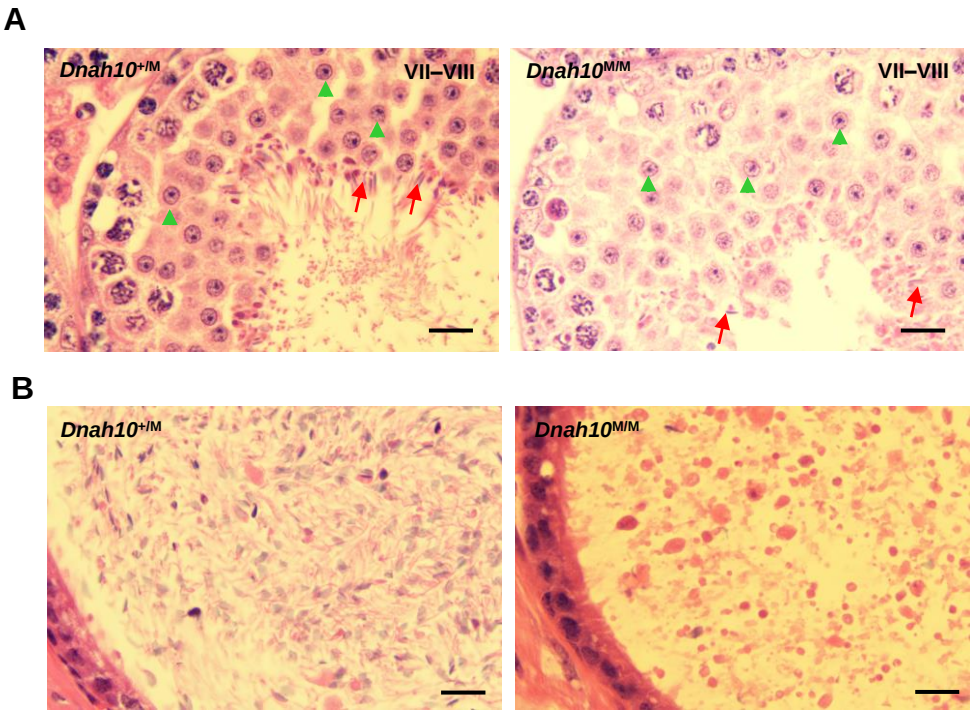

Figure S12. Histological Examinations of Testes and Epididymides from *Dnah10*$^{+/M}$ and *Dnah10*$^{M/M}$ Male Mice

(A) H&E staining of testicular tissues in *Dnah10*$^{M/M}$ male mice and *Dnah10*$^{+/M}$ male mice at 7 weeks old. In stage VII–VIII seminiferous tubules from *Dnah10*$^{M/M}$ male mice, normal round spermatids (green, arrowheads) were observed, but the morphology of elongated tails (red arrows) were abnormal. Scale bars = 20 μm.

(B) H&E staining of epididymal sections in *Dnah10*$^{M/M}$ male mice and *Dnah10*$^{+/M}$ male mice at 7 weeks old. Compared with *Dnah10*$^{+/M}$ male mice, sperm counts were obviously decreased in the epididymis from *Dnah10*$^{M/M}$ male mice. Scale bars = 20 μm.

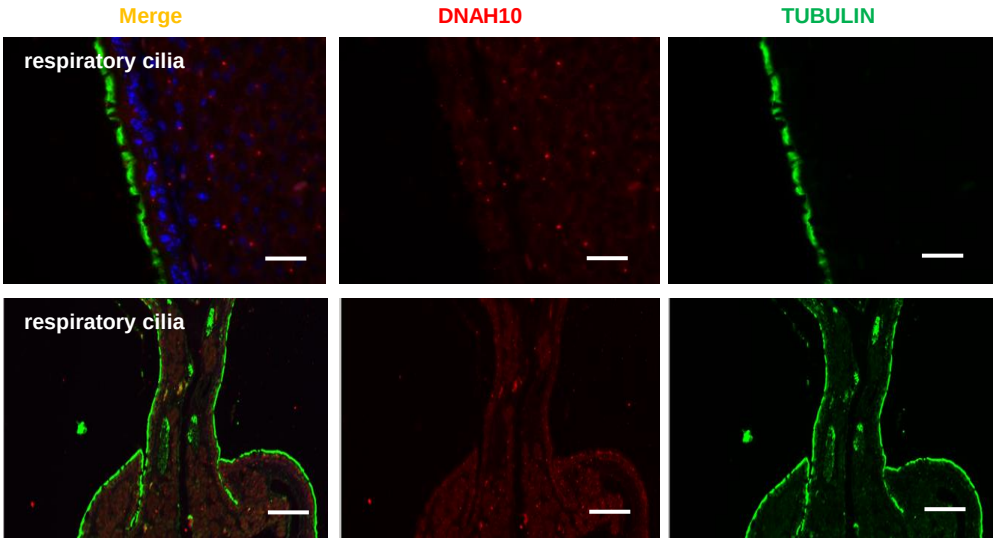

Figure S13. Immunofluorescence Staining of DNAH10 in the Respiratory Cilia from a Fertile Male Control.

Respiratory cilia cells were stained with anti-DNAH10 (red) and anti-α-tubulin (green) antibodies. DNA was counterstained with DAPI as a marker of the cell nucleus. DNAH10 staining using the antibody recognizing the C-terminus of DNAH10 (amino acids 3561-3700) is not detectable at the respiratory cilia. Scale bars = 20 μm.

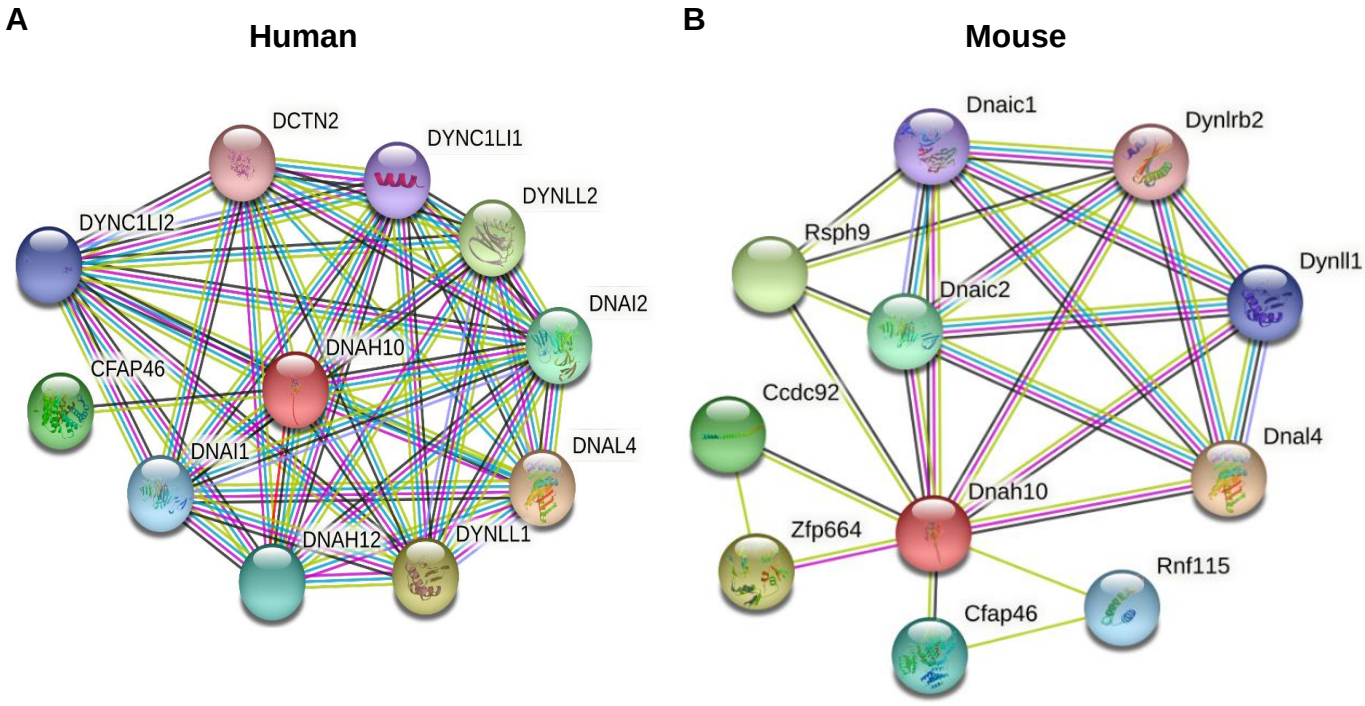

Figure S14. The Protein-Protein Interactions for DNAH10/Dnah10 Predicted by STRING.

The protein interaction networks were predicted using *in silico* software String for human and mouse DNAH10/Dnah10 proteins, respectively. The direct interaction was predicted between human DNAH10 and DYNLL2, DYNC1LI2 and DYNC1LI2, but no direct interaction was shown between mouse Dnah10 and Dynll2, Dync1li2 and Dync1li2. The yellow lines suggest the interactions using text mining, and black lines indicate the identification of co-expression.

Table S1. Primers Used for Verification of *DNAH10* Variants

Primer name	F/R	Primer Sequence (5' to 3')	Annealing Temperature (℃)
DNAH10 (c.G12838A)	F1	GGATGACGAAGTCTCTGGCTG	57
	R1	CTAGGCTGACACCTGAATCGG	
DNAH10 (c.7601C>T)	F2	AAACTGAAACCGAGGTGCCC	58
	R2	CTTGGGTCAACTTCATTGCGG	
DNAH10 (c.5663G>A)	F3	GGCTGGTCACCTGCTT	51
	R3	CCACGCCCATTCATAAC	
DNAH10 (c.11887C>T)	F4	CCCGACTTCCTGGTG	48
	R4	AGCGGCTCCCTCTAA	
DNAH10 (c.7260dup)	F5	CATCTGTCCAGTGATGAG	55
	R5	GCATCTCATCTGCCTGTGG	
DNAH10 (c.12235del)	F6	GATTGGCTGGAACGTGTACTA	56
	R6	GGAATTGATGTCACTGCC	

Abbreviation: F, forward primers; R, reverse primers.

Table S2. Primers Used for Mouse *Dnah10* Genotyping

Primer name	F/R	Primer Sequence (5' to 3')	Annealing Temperature (℃)	Length (bp)
Dnah10-KO	F1	GGTGCCTTCACTCTGTAAGTGTC	60	791
	R1	GCTGTCTGTTACACTGATGGATG		
Dnah10-KO	F2	GGTGCCTTCACTCTGTAAGTGTC	60	622
	R2	GCTTCATTTCCTCCAGACACCC		
Dnah10-KI	F3	CTGGTGGTTGGAGGTAGCTTT	58	342
	R3	CTGGAAGAAATCATCATAGGAG		

Abbreviation: F, forward primers; R, reverse primers; KO, knockout. KI, knockin.

Table S3. Primers Used for RT-PCR Assays

Primer name	F/R	Primer Sequence (5' to 3')	Annealing Temperature (℃)	Length (bp)
Dnah10-1 (Exons 1-6)	F1	AACCTCACCAACCCTATGCT	55	732
	R1	ATCGCGGATCAGTTGGACG		
Dnah10-KO (Exon 4-7)	F2	TTCAAAAGACGCCATCCCAGAA	57	448
	R2	GATCACGCACTGCTCCAAAT		
Dnah10-2 (Exon 38-40)	F	TTATGTGCTCCTGCCAGTCC	57	371
	R	TGTTGTCGTCCATCACGGAG		
Dnah10-3 (Exon 46-48)	F	GAACATGCCAAAGGTGGATGAG	57	237
	R	TTCAGGGACTCCTCCGATGG		
Dnah10-4 (Exons 71-75)	F	TGACTTCCAGGTCTGTATGGAAAT	56	422
	R	TGCTGGACTCCCCTGTCTG		
Gapdh (RT-PCR in Mice)	F	GGTGAAGGTCGGTGTGAACG	57	233
	R	CTCGCTCCTGGAAGATGGTG		

Abbreviation: F, forward primers; R, reverse primers; KO, knockout.

Table S4. Semen Routine Parameters and Sperm Flagellar Morphology in Men Harboring Bi-allelic *DNAH10* Variants

Subject	T012 II-2	T089 II-1	H049 II-2	NK067 II-1	NK067 II-2	Reference Limits
Semen Parameter						
Semen volume (mL)	6.7	3.3	2.0	3.7	2.6	>1.5[a]
Sperm concentration (10^6/mL)	1.6*	0.5*	6.6*	71.2	72.6	>15.0[a]
Motility (%)	0*	0*	9.2*	10.3*	11.8*	>40.0[a]
Progressive motility (%)	0*	0*	1.7*	1.9*	2.4*	>32.0[a]
Sperm Flagella Morphology						
Absent flagella (%)	3.6	12.0*	11.8*	24.5*	4.5	<5.0[b]
Short flagella (%)	29.0*	21.0*	8.8*	15.6*	9.1*	<1.0[b]
Coiled flagella (%)	38.5*	45.0*	41.2*	38.1*	58.3*	<17.0[b]
Angulation (%)	7.5	3.5	30.9*	6.1	3.8	<13.0[b]
Irregular caliber (%)	8.0*	5.5*	2.9*	4.1*	2.3*	<2.0[b]

[a]Reference limits according to the WHO standards.[43]

[b]Reference limits according to the distribution range of morphologically normal spermatozoa observed in 926 fertile individuals.[44]

*Abnormal value

Table S5. Rates of Ultrastructural Abnormalities in the Spermatozoa from Men Harboring Bi-allelic *DNAH10* Variants.

Subject	Control [a] (n=45)	T012 II-2 (n=30)	NK067 II-1 (n=25)	NK067 II-2 (n=45)
Missing IDA	0 (0%)	15 (50.0%)	18 (72.0%)	31 (68.9%)
Missing CP	1 (2.2%)	1 (3.3%)	0 (0%)	2 (4.4%)
Missing MT	4 (8.9%)	6 (20.0%)	0 (0%)	1 (2.2%)
Global disorganization	1 (2.2%)	3 (10.0%)	0 (0%)	4 (8.9%)

[a] Values represent the mean of three normal males; n, number of cross sections for analysis.

Abbreviations: IDA, inner dynein arms; CP, central pair of microtubules; MT, peripheral microtubule doublet.

Table S6. Sperm Morphology in *Dnah10*-Mutated Male Mice [a]

	***Dnah10*$^{+/+}$**	***Dnah10*$^{-/-}$**	***Dnah10*$^{M/M}$**
Sperm Morphology [b]			
Absent flagella (%)	3.5 ± 0.4	13.5 ± 0.6	10.5 ± 0.5
Short flagella (%)	0.3 ±0.9	22.3 ±0.5	25.3 ±0.7
Coiled flagella (%)	2.1 ± 0.5	40.6 ± 0.7	37.6 ± 0.5
Irregular caliber (%)	0.9 ± 1.1	12.9 ± 0.9	16.9 ± 0.6
Bent flagella (%)	1.7 ± 0.7	10.7 ± 0.5	9.7 ± 0.7

a Values represent the mean (range).

b Per single epididymis.

Table S7. Clinical Outcomes of ICSI Cycles Using the Spermatozoa from Men Harboring Bi-allelic *DNAH10* Variants

Subject	T012 II-2	H049 II-2	NK067 II-2
Male age (year)	30	37	38
Female age (year)	30	29	34
Number of ICSI cycles	1	1	1
Number of oocytes injected	11	6	15
Number (and rate) of fertilized oocytes	9(82%)	5(83%)	12(80%)
Number (and rate) of cleavage embryos	9(100%)	5(100%)	12(100%)
Number (and rate) of 8-cells	6(66%)	4(80%)	10(83%)
Number (and rate) of blastocysts	6(66%)	3(60%)	9(75%)
Number of transfer cycles	1	1	1
Number of embryos transferred per cycle	2	2	2
Implantation rate	50%	0	50%
Clinical pregnancy rate	100%	NA	100%
Miscarriage rate	NA	NA	NA

NA, not available.